

Statistics of Wave Orbital Velocities in Random Directional Sea States

A. Alberello¹, A. Chabchoub¹, O. Gramstad¹, A. Babanin¹ and A. Toffoli¹

¹Centre of Ocean Engineering Science and Technology
Swinburne University of Technology, Hawthorn, Victoria 3122, Australia

Abstract

The inclusion of at least the second order nonlinear contribution is necessary to achieve an accurate representation of ocean waves. While this is well known for the surface elevation, the importance of second order nonlinearity on the velocity potential, and hence on the wave kinematics and associated wave loads, is still unclear. To explicitly address the effect of nonlinear contribution on wave velocities Monte-Carlo simulations with a second order wave model are carried out with different initial random conditions. Results show that the statistical distribution of the horizontal components of wave orbital velocity departs substantially from Normality due to second order contributions for both unidirectional and directional wave fields.

Introduction

Offshore structures have to withstand extreme loads due to the wave action. Together with a reliable estimation of the probability of occurrence of freak waves in a stormy sea, the maritime industry also requires enhanced estimation of the wave loads associated to extreme waves. Wave forces on offshore structures are usually estimated as a function of wave-induced velocities by the Morison equation [5]

$$F = \rho C_m V \dot{u} + \frac{1}{2} \rho C_d A u |u|, \quad (1)$$

where C_m and C_d are the inertia and drag coefficient, A and V are the frontal area and the body volume, ρ is the water density and u is the horizontal velocity component of the wave orbital motion with \dot{u} its derivative. Thus, correct reconstruction of the velocity field below water waves assumes a fundamental role in the evaluation of the intensity of the wave-structure interaction. Due to its practical implications the wave kinematics have been deeply investigated (e.g. [1] and references therein) to fully characterize the velocity field and hence the wave induced loads on structures.

Mathematically, the wave motion problem can be fully represented by the boundary value problem described by the laplacian of the velocity potential ϕ

$$\nabla^2 \phi = 0, \quad (2)$$

and its boundary conditions:

$$\frac{\partial \phi}{\partial z} = 0, \quad (3)$$

$$\frac{\partial \eta}{\partial t} + u \frac{\partial \eta}{\partial x} + v \frac{\partial \eta}{\partial y} = w, \quad (4)$$

$$g\eta + \frac{1}{2}(u^2 + v^2 + w^2) + \frac{\partial \phi}{\partial t} = -Q(t), \quad (5)$$

equation (3) is the no flow condition at the bottom, equations (4) and (5) are respectively the kinematic and dynamic (nonlinear) condition at the free surface. Q is the Bernoulli term, g the gravity constant, t the time, u , v and w the velocity components

along x , y and z respectively, z is positive upwards with zero at the mean water level.

Explicit analytical solution at the leading order for the water surface and velocity field are based on a linear superposition of sinusoidal components, which can only reproduce small amplitude wave conditions. Higher order effects are completely disregarded and hence representations of more extreme waves, where wave-wave nonlinear interaction play a more substantial role, are not accurate.

A second order expansion of the water wave problem is routinely used by offshore and shipping industry to include nonlinear contributions. For the surface elevation, this results in an interaction between wave components, which leads to a sharpening of wave crests and flattening of wave troughs. For random wave fields, this means that wave crest and wave troughs distributions depart from standard linear distribution such as the Rayleigh distribution [9, 2, 10, 11, 12], leading to an increase of probability of extreme wave events. While the effect of the nonlinear contribution on the surface elevation is fully understood, fewer investigations have been conducted to address the effect of second on the probability density function associated to the wave-induced velocities.

Second order solutions for monochromatic waves [4], in this respect, indicates that nonlinear contribution to wave kinematics vanishes when the water depth is infinite (i.e. waves do not feel the bottom). This case, however, is only limited to the interaction of a wave with itself. Thus it is not yet completely clear what role the nonlinear interaction between different wave components play on wave-induced velocities.

Here we obtain the wave kinematics using an approximate solution of the equation (2) up to the second order [7] that allows an accurate reconstruction of most of the wave nonlinearities observed in physical experiments [6, 13, 8]. Monte-Carlo simulations of unidirectional and directional JONSWAP sea-states are generated to explicitly analyze the effects of the second order nonlinear effects on the velocity in deep water conditions.

Simulation Method

Numerical Method

The classical second-order theory for water waves [7] provides explicit expressions for the second order surface elevation $\eta(x, y, t)$ and second order velocity potential $\phi(x, y, z, t)$. Both the velocity potential and the water elevation can be written as a sum of linear and second order contribution

$$\phi = \phi^{(1)} + \phi^{(2)}, \quad (6)$$

$$\eta = \eta^{(1)} + \eta^{(2)}, \quad (7)$$

where the linear terms are respectively

$$\phi^{(1)}(\mathbf{x}, z, t) = \sum_{i=1}^{\infty} \frac{a_i g}{\sigma_i} \frac{\cosh k_i(h+z)}{\cosh k_i h} \sin(\psi_i), \quad (8)$$

$$\eta^{(1)}(x, y, t) = \sum_{i=1}^{\infty} a_i \cos(\psi_i), \quad (9)$$

where a is the wave amplitude, g the gravity constant, h the water depth, σ the angular frequency, k the wavenumber and ψ is defined as

$$\psi_i(x, y, t) = \mathbf{k}_i \mathbf{x} - \sigma_i t + \varepsilon_i, \quad (10)$$

with $\mathbf{k} = (k_x, k_y)$, $\mathbf{x} = (x, y)$ and ε the phase.

The second order contribution can be written as a sum of a positive ($\eta^{(2+)}, \phi^{(2+)}$) and a negative contribution ($\eta^{(2-)}, \phi^{(2-)}$) such that

$$\phi^{(2)} = \phi^{(2-)} + \phi^{(2+)}, \quad (11)$$

$$\eta^{(2)} = \eta^{(2-)} + \eta^{(2+)}. \quad (12)$$

The expressions for the second order contribution to the velocity potential and the wave elevation are respectively:

$$\phi^{(2\pm)} = \frac{1}{4} \sum_{i=1}^{\infty} \sum_{j=1}^{\infty} \frac{a_i a_j g^2 \cosh k_{ij}^{\pm} (h+z)}{\sigma_i \sigma_j \cosh k_{ij}^{\pm} h} P_{ij}^{\pm} \sin(\psi_i \pm \psi_j), \quad (13)$$

$$\eta^{(2\pm)} = \frac{1}{4} \sum_{i=1}^{\infty} \sum_{j=1}^{\infty} a_i a_j N_{ij}^{\pm} \cos(\psi_i \pm \psi_j). \quad (14)$$

The kernel functions P_{ij}^{\pm} and N_{ij}^{\pm} are defined as:

$$P_{ij}^{\pm} = \frac{D_{ij}^{\pm}}{\sigma_i \pm \sigma_j}, \quad (15)$$

$$N_{ij}^{\pm} = \left[\frac{D_{ij}^{\pm} - (\mathbf{k}_i \mathbf{k}_j \mp R_i R_j)}{\sqrt{R_i R_j}} + (R_i + R_j) \right] \cos(\psi_i \pm \psi_j), \quad (16)$$

where

$$D_{ij}^{\pm} = \left(\frac{(\sqrt{R_i} \pm \sqrt{R_j}) [\sqrt{R_j} (k_i^2 - R_i^2) \pm \sqrt{R_i} (k_j^2 - R_j^2)]}{(\sqrt{R_i} \pm \sqrt{R_j})^2 - k_{ij}^{\pm} \tanh k_{ij}^{\pm} h} \right) + \left(\frac{2(\sqrt{R_i} \pm \sqrt{R_j})^2 (\mathbf{k}_i \mathbf{k}_j \mp R_i R_j)}{(\sqrt{R_i} \pm \sqrt{R_j})^2 - k_{ij}^{\pm} \tanh k_{ij}^{\pm} h} \right), \quad (17)$$

and

$$R_i = |\mathbf{k}_i| \tanh |\mathbf{k}_i| h, \quad (18)$$

$$k_{ij}^{\pm} = |\mathbf{k}_i \pm \mathbf{k}_j|. \quad (19)$$

Initial Conditions

Monte-Carlo simulations are performed for realistic random unidirectional and directional sea-state conditions. As underlying spectral distribution for the linear solution a JONSWAP spectrum has been used

$$E(k) = \frac{\alpha}{2} \frac{1}{k^4} \exp \left[-\frac{5}{4} \left(\frac{k_p}{k} \right)^2 \right] \gamma^{-\exp(\sqrt{k-k_p-1})^2 / (2s^2)} \quad (20)$$

where E is the wave energy, k_p is the peak wavenumber, s ($s = 0.09$ if $k < k_p$, $s = 0.07$ elsewhere), γ and α are parameters that control the shape and peak enhancement of the spectrum. Simulations are performed for $\gamma = 6$ while α is chosen in order to achieve storm-wave conditions ($k_p a \approx 0.16$). For the directional wave field a cosine squared spreading function $\cos^{2N}(\theta)$ is adopted, a wide directional spectrum is obtained setting N equal to 1.

Deep water condition is considered in the simulations (relative water depth $kd = \infty$). Monte-Carlo simulations are carried out by generating 1000 realizations with random phase and random amplitude approximation. The phase is uniformly distributed,

while the amplitude obeys to a Rayleigh distribution. Computations first evaluate the linear approximation of an initial surface and then add second order corrections. A spatial domain discretized by 512 elements is used. The spatial resolution is chosen to have at least 20 points per dominant wavelength so that about 24 dominant waves are included in the domain. A reduced grid size (128×128) and a lower number of realizations (200) have been used for the more computationally intense two dimensional cases. In this regard, it is worth mentioning that one realization of a unidirectional wave field requires a cpu time of 0.6s. For the two-dimensional case the cpu time is substantially larger and overcomes 900s per realization.

The horizontal velocity $\mathbf{u}(\mathbf{x}, z, t)$, which is the spatial derivative of the potential ϕ , can then be easily and efficiently be computed in the Fourier space

$$\mathbf{u}(\mathbf{x}, z, t) = \mathcal{F}^{-1} \{ i \mathbf{k} \mathcal{F} [\phi(\mathbf{x}, z, t)] \}. \quad (21)$$

Results

To better understand the effect of second order contribution on wave kinematics, monochromatic and bi-chromatic waves and their second order components are presented in figure 1.

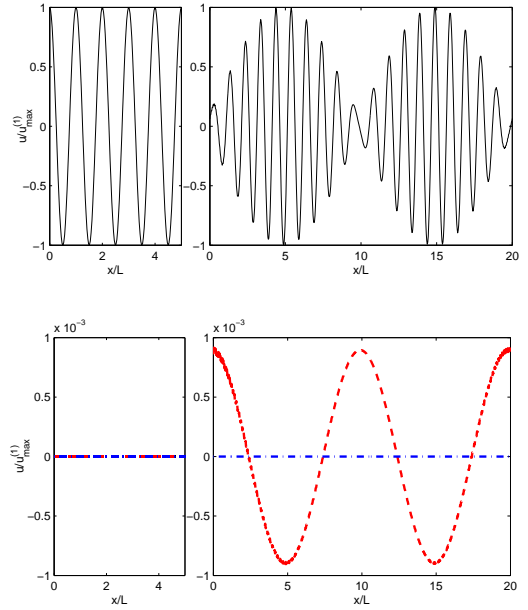


Figure 1. Non-dimensional velocity versus the non-dimensional space at water depth $d = L/6$. Left panels monochromatic wave ($ka = 0.16$), right panels bi-chromatic wave ($k_1 = 0.95 \cdot k$, $k_2 = 1.05 \cdot k$ and $a_1 = a_2 = a/2$). Top panels linear contribution $u^{(1)}$ (—), lower panels second order terms $u^{(2-)}$ (---), $u^{(2+)}$ (-.-).

In the top-left panel of figure 1 the linear contribution for a monochromatic wave is shown: $u^{(1)}$ is a sinusoidal signal. Both the $u^{(2-)}$ and $u^{(2+)}$ vanish in deep water as predicted by second order theory (bottom-left panel in figure 1). Right panels show the case of a bi-chromatic wave spectrum with the two wave components closely spaced ($\Delta k = 0.1 \cdot k$). In this case the first order contribution results from the linear superposition of the two wave components (top-right panel in figure 1). As in the case of monochromatic waves the positive term $u^{(2+)}$ vanishes

also for bi-chromatic waves, while the negative contribution oscillates with a wavelength equal to the length of the wave group with nodes at the beginning and in the middle of the wave group $u^{(1)}$.

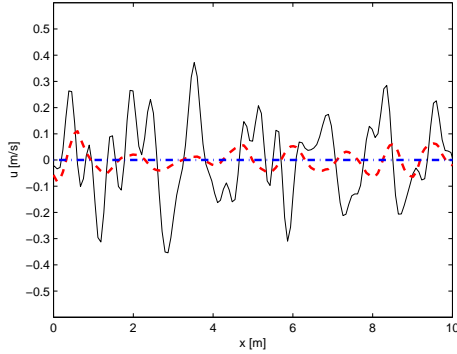


Figure 2. Example velocity versus the space at water depth $d = L/6$. $u^{(1)}$ (—), $u^{(2^-)}$ (---), $u^{(2^+)}$ (-·-·).

An example of the velocity potential obtained from equations (8) and (13) for one of the Monte-Carlo realizations of the JONSWAP spectrum is shown in figure 2. The second order contribution $u^{(2^+)}$ vanishes in deep water conditions, as it have been observed for monochromatic and bi-chromatic wave spectra. Also in a random sea-state the velocity is strongly affected by the negative contribution, $u^{(2^-)}$, analogously to the case of a bi-chromatic waves.

In figure 3 the linear contribution $u^{(1)}$ computed from the Monte-Carlo simulation is close to the Gaussian distribution which is the theoretical distribution for the linear solution. In deep water condition the positive contribution ($u^{(2^+)}$) has no effect on the linear contribution while the negative second order correction ($u^{(2^-)}$) sensibly increases the absolute value of the negative tail while the positive tail remains almost not affected by the nonlinear contribution. Adding the second order contribution the probability density function becomes left-skewed beneath the surface and for a probability of 10^{-4} the nonlinear velocity is about 25% higher than the linear solution. Analogous deviation has been observed for both the directional sea-state (bottom panel figure 3) despite the deviation towards negative values is less intense in this case. The wave directionality seems to have little effect on the statistical distribution of the second order velocities.

Conclusions

Monte-Carlo simulations of random unidirectional and directional sea-states up to the second order have been performed with a second order wave model [7] to assess the effect of wave nonlinearity on the velocity potential and wave-induced velocity. Initial conditions were imposed by a JONSWAP spectrum with a $\cos^N(\theta)$ directional function. Only deep water conditions were investigated.

Second order contribution strongly affects the probability density function of the wave velocities below the surface. When nonlinear terms are included there is a strong deviation of the negative tail of the velocity distribution: for the probability 10^{-4} the velocity is about 25% higher than the velocity predicted by the linear theory. This relevant deviation from first order theory is mainly due the $u^{(2^-)}$ term. Higher negative velocity has also been measured [6], despite they suggest that this is caused by the return flow in intermediate water depth we be-

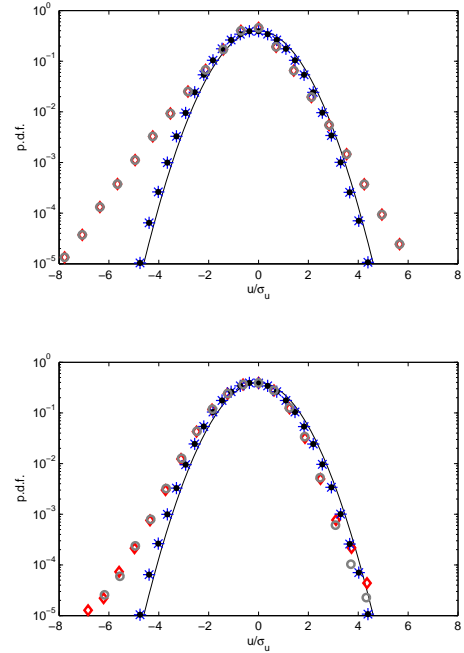


Figure 3. Probability density function of the horizontal velocity at water depth $d = L/6$ for unidirectional sea-states (top-panel) and directional seas (lower panel). Gaussian distribution (—), $u^{(1)}$ (●), $u^{(1)} + u^{(2^-)}$ (◇), $u^{(1)} + u^{(2^+)}$ (*), $u^{(1)} + u^{(2^-)} + u^{(2^+)}$ (○).

lieve that is purely due to the second order contribution. Physical experiments in a large experimental facility [12] and the second order approach adopted by both [8] and us leads to the same results for intermediate and deep water conditions. Wave directionality seems not to have any effect on the potential and the velocity in deep water condition, higher order terms may be affected by wave directionality.

The significant increase of the wave velocity below the surface means that the wave loads on offshore structure are sensibly higher than the forces that can be predicted with a purely linear approach. Inclusion of second order term in the velocities calculation may affect the design criteria of offshore platform.

References

- [1] Grue, J., Clamond, D., Huseby, M. and Jensen, A., Kinematics of Extreme Waves in Deep Water, *Applied Ocean Research*, **25**, 2003, 355–366.
- [2] Forristall, G. Z., Wave Crest Distributions: Observations and Second-Order Theory, *Journal of Physical Oceanography*, **30**, 2000, 1931–1943.
- [3] Hasselmann K., Barnett, T.P., Bouws, E., Carlson, H., Cartwright, D.E., Enke, K., Ewing, J.A., Gienapp, H., Hasselmann, D.E., Kruseman, P., Meerburg, A., Miller, P., Olbers, D.J., Richter, K., Sell, W. and Walden, H., Measurements of Wind-Wave Growth and Swell Decay During the Joint North Sea Wave Project (JONSWAP), *Ergänzung zur Deut. Hydrogr. Z., Reihe A (8)*, **12**, 1973, 1–95.

- [4] Longuet-Higgins, M.S., The Effect of Non-Linearities on Statistical Distributions in the Theory of Sea Waves, *Journal of Fluid Mechanics*, **17**, 1963, 459–480.
- [5] Morison, J.R., Johnson, J.W. and Schaaf, S.A., The Force Exerted by Surface Waves on Piles, *Journal of Petroleum Technology*, **2**, 1950, 149–154.
- [6] Ning, D., Zang, J., Liu, S., Eatock Taylor, R., Teng, B. and Taylor, P., Free-Surface Evolution and Wave Kinematics for Nonlinear Uni-Directional Focused Wave Groups, , *Ocean Engineering*, **36**, 2009, 1226–1243.
- [7] Sharma, J.N. and Dean, R.G., Second Order Directional Seas Surface and Associated Wave Forces, *Society of Petroleum Engineers Journal*, **21**, 1981, 129–140.
- [8] Song, J.B. and Wu, Y.H., Statistical Distribution of Water-Particle Velocity Below the Surface Layer for Finite Water Depth, *Coastal Engineering*, **40**, 2000, 1–19.
- [9] Tayfun, M.A., Narrow-Band Nonlinear Sea Waves, *Journal of Geophysical Research*, **85**, 1980, 1548–1552.
- [10] Toffoli, A., Benoit, M., Onorato, M. and Bitner-Gregersen, E., The Effect of Third-Order Nonlinearity on Statistical Properties of Random Directional Waves in Finite Depth, *Nonlinear Processes in Geophysics*, **16**, 2009, 131–139.
- [11] Toffoli, A., Gramstad, O., Trulsen, K., Monbaliu, J., Bitner-Gregersen and E. Onorato, M., Evolution of Weakly Nonlinear Random Directional Waves: Laboratory Experiments and Numerical Simulations, *Journal of Fluid Mechanics*, **664**, 2010, 313–336.
- [12] Toffoli, A., Fernandez, L., Monbaliu, J., Benoit, M., Gagnaire-Renou, E., Lefèvre, L., Cavaleri, L., Proment, D., Pakodzi, C., Stansberg, C.T., Waseda and Onorato, M., T. Experimental Evidence of the Modulation of a Plane Wave to Oblique Perturbations and Generation of Rogue Waves in Finite Water Depth, *Physics of Fluids*, **25**, 2013, 091701.
- [13] You, Z.J., The Statistical Distribution of Nearbed Wave Orbital Velocity in Intermediate Coastal Water Depth, *Coastal Engineering*, **56**, 2009, 844–852.